Vertical partitioning and controlling factors of gradient-based soil carbon dioxide fluxes in two contrasted soil profiles along a loamy hillslope.

Authors : Wiaux, F. [†*], Vanclooster, M. [†], Van Oost, K.[‡**]

† Environmental Sciences, Earth& Life Institute, Universitécatholique de Louvain, Croix du Sud 2, 1348 Louvain-la-Neuve, Belgium; ‡ George Lemaître Centre for Earth and ClimateResearch, Earth& Life Institute, Université Catholique de Louvain, Place Louis Pasteur 3, 1348 Louvain-la-Neuve, Belgium ; ** Fonds National pour la Recherche Scientifique (FNRS), Belgique.

Authors email addresses:

francois.wiaux@uclouvain.be, marnik.vanclooster@uclouvain.be, kristof.vanoost@uclouvain.be.

* Corresponding author:

E-mail address: francois.wiaux@gmail.com;

Phone number: 0032(0)10473712

Full postal address: Earth& Life Institute, Université catholique de Louvain, Croix du Sud n°2, BP L7.05.02, 1348, Louvain-la-Neuve, Belgium

Key words: C dynamic model; CO_2 flux; physical control; vertical partitioning; OC storage; Hillslope; cropland; loess soil.

Type of paper: Regular research paper

Abstract

In this study, we aim to elucidate the role of physical conditions and gas transfer mechanism along soil profiles in the decomposition and storage of soil organic carbon (OC) in subsoil layers. We use a qualitative approach showing the temporal evolution and the vertical profile description of CO_2 fluxes and abiotic variables. We assessed soil CO_2 fluxes throughout two contrasted soil profiles (i.e. summit and footslope positions) along a hillslope in the central loess belt of Belgium. We measured time-series of soil temperature, soil moisture and CO_2 concentration at different depths in the soil profiles for two periods of 6 months. We then calculated the CO_2 flux at different depths using Fick's diffusion law and horizon specific diffusivity coefficients. The calculated fluxes allowed assessing the contribution of different soil layers to surface CO_2 fluxes. We constrained the soil gas diffusivity coefficients using direct observations of soil surface CO_2 fluxes from chamber-based measurements and obtained a good prediction power of soil surface CO_2 fluxes with a R^2 of 92%.

We observed that the temporal evolution of soil CO_2 emissions at the summit position is mainly controlled by temperature. In contrast, at the footslope, we found that long periods of CO_2 accumulation in the subsoil alternates with short peaks of important CO_2 release. This was related to the high water filled pore space that limits the transfer of CO_2 along the soil profile at this slope position. Furthermore, the results show that approximately 90 to 95 % of the surface CO_2 fluxes originate from the first 10 centimeters of the soil profile at the footslope. This indicates that soil OC in this depositional context can be stabilized at depth, i.e. below 10 cm. This study highlights the need to consider soil physical properties and their dynamics when assessing and modeling soil CO_2 emissions. Finally, changes in the physical environment of depositional soils (e.g. longer dry periods) may affect the long-term stability of the large stock of easily decomposable OC that is currently stored in these environments.

1. Introduction

Soils play a major role in the global C budget, as they contain 2 to 3 times more C than the atmosphere (Eswaran et al., 1993; Lal et al., 2003). However, current assessments of the exchange of C between the soil and the atmosphere in response to environmental change are associated with large uncertainties (e.g. Peters et al., 2010). One of the sources of this uncertainty is related to our poor understanding of C dynamics in the deeper layers of the soil profile. Rumpel and Kögel-Knabner (2011) showed that deep soil OC is highly processed, but that subsoil C fluxes from C input, stabilization and destabilization processes are still poorly constrained. In addition to this, recent work has highlighted the significance of buried OC in depositional setting for the C cycle (e.g. Berhe et al 2007; Van Oost et al., 2012; Wang et al., 2014; Wiaux et al., 2014). More specifically, buried OC that is stored in colluvial soils at the bottom of eroding hillslopes (e.g. Stallard et al., 1998)cannot be assumed to be inert to loss as it can decompose as a result of continued degradation or disturbances such as global warming, desiccation of saturated soils, land use change, and re-excavation by gullying (e.g. Van Oost et al., 2012). Somes studies suggested an “erosion-induced C source” along hillslope ranging from 0.37 petagram C per year (Jacinthe and Lal 2001) to 0.8-1.2 petagram C per year (Lal 2003). This shows that more quantitative information on the contribution of deep C to soil-atmosphere C exchange as well an increased understanding of the controlling factors is needed.

There is now significant concern about the contribution of soil organic carbon (OC) to future climate change where a climate change driven acceleration of soil OC decomposition could represent a positive feedback on climate (e.g. Davidson and Janssens, 2006; Frey et al., 2013). Under our temperate climate, temperature increase as well as summer drought would constitute potential climatic changes (IPCC, 1990; 1992) which are supposed to increase OC turnover (e.g. Davidson and Janssens, 2006).

Recent studies highlight the importance of soil bio-physical conditions that may vary substantially with time and across landscapes (e.g. Dai et al., 2012). These studies have shown that, in addition to the effects of soil moisture, temperature and OC quality, soil physical properties (e.g. gas diffusion barriers) may also exert an important control on soil microbial activity and soil CO_2 fluxes (e.g. Wiaux

et al., 2014b; Ball, 2013; Maier et al., 2011). Furthermore, there is empirical evidence suggesting that physical protection (i.e. soil aggregates) is a key factor controlling the long-term stability of OC in soils (e.g. Schmidt et al., 2011). Schmidt et al.(2011) also argued that physical conditions may prevent decomposition of deep OC even if this OC would be easily decomposable under optimal conditions. However, other process studies indicate that subsoil OC represents an important C store that interacts actively with the atmosphere (e.g. Rumpel and Kögel-Knabner, 2011). Understanding the soil physical controls on soil CO_2 fluxes is thus particularly relevant in landscapes with complex topography where buried OC in depositional areas represent a significant part of the total OC stored(e.g. Van Oost et al., 2012; Wang et al., 2014 and Wiaux et al., 2014a).

In a forest ecosystem, Goffin et al. (2014) showed that the upper first 30centimeters of a soil profile contribute substantially to the total surface CO_2 flux. However, to our knowledge, a vertical partitioning has not been evaluated in agro-ecosystems or in systems with contrasting soil physical and/or chemical properties. Agro-ecosystems differ from forest ecosystems as litter and A horizons in forest ecosystems are characterized by both a high amount and quality of OC (e.g. Brahy et al., 2002; Goffin et al., 2014), while these horizons have disappeared in crop soils due to erosion, plowing, and export of plant residues (e.g.Wiaux et al., 2014a). Hence, deep OC in forest soils may have a lower contribution relatively to surface CO_2 fluxes given that surface soil horizons enriched in fresh organic matter are more likely to emit more CO_2thansoils in croplands. In addition, roots network in forests is dense and difficult to remove when installing in situ measurement settings compared to cropsoils. This creates interferences when measuring heterotrophic CO_2 fluxes as an indicator of OC turnover (e.g. Davidson et al., 1998; Epron et al., 2006; Fiener et al., 2012).

In this study, we aim to elucidate the role of physical controls on soil-atmosphere CO_2 fluxes and its variation with soil depth for a cultivated soil. To this aim, we present a comparative analysis between two contrasting soil profiles along an eroded and cultivated hillslope. Previous work (i.e. Wiaux et al., 2014b), has shown that soil surface CO_2 respiration is highly variable along this hillslope, with 30% more respiration at the downslope and 50% more at the backslope, relative to the uneroded summit position. Why some controlling factors have been identified, the role of soil physical controls and of

the significance of subsoil OC contributions remain unkown. The specific objectives of this study are then: (i) to quantify the relative contribution of soil surface and subsoil OC to CO_2 fluxes through a vertical partitioning of these fluxes; and (ii) to identify the role of soil physical properties using time-series of soil moisture measurements and gas diffusivity at different depths. The selected study site is characterized by two contrasting soils in terms of soil hydrological regimes and soil structure and is representative for the cultivated soils of the Belgian loam belt.

2. Material and methods

2.1. Study site description

The study was carried out in the Belgian loam belt along a cultivated hillslope of 150 meters length (50.6669°N, 4.6331° W). The site has a maritime temperate climate, with an average annual temperature of 9.7°C and an average annual precipitation of 805 mm. The slope percentage in the backslope area ranges between 8.5 and 16%, with a mean slope of 12%. The slope percentage in the convex shoulder area ranges between 4 to 8.5%, with an average of 6%. The field was plowed (0-30 cm soil surface layer) every year. Each year, manure and nitrate fertilization was carried out. The previous crop rotation was winter wheat, maize and spring wheat. The study site has been described in detail in Wiaux et al. (2014a,b). For this study, we selected two measurement stations along the hillslope: one at the summit and one at the footslope position. The soil is a Dystric Luvisol type at the summit and a Colluvic Regosol in the depositional area at the footslope (IUSS Working Group WRB, 2007; Wiaux et al., 2014a,b).

2.2. Soil physical and bio-chemical properties

In order to characterize the physical and bio-chemical properties of these two soil profiles, we measured soil porosity and soil water retention (SWR) curves. Total OC, labile OC and soil porosity were already characterized by Wiaux et al. (2014 a,b) and are illustrated in Fig. 1. Total C (i.e. the sum of organic and inorganic C) was analyzed using an elemental analyzer (Variomax, Elementar GmbH). Instrument precision for total C analyses is 0.05% C concentration. The samples were then treated with 1% HCl in order to remove inorganic CaCO3 and were analyzed again with the elemental

analyzer. Soil OC concentration was then deduced from the difference between total carbon analyses before and after 1% HCl treatments. Stable OC was defined as the pool of NaOCl-resistant OC (Siregar et al., 2005). We quantified the stable OC by mixing 3 g of air dried soil with 30 ml of 6 wt % NaOCl (adjusted to pH 8). The NaOCl-treated soil was then washed (shaken and centrifuged) with de-ionized water until the solution was chloride free (i.e. no reaction with AgNO3 occurred). The samples were then dried at 105°C and homogenized before collecting a subsample for total C measurement by dry combustion. The labile OC pool was defined as the residual OC pool that was not resistant to NaOCl oxidation. Hence, this labile OC pool should be interpreted as easily mineralizable OC under ideal conditions where no other factors play a role in stabilization (e.g. anoxic environment, aggregation, etc).

The total porosity (Ǿ) was already characterized by Wiaux et al. (2014a,b) and is illustrated in Fig. 2 Porosity was measured in the laboratory by weighing 100 cm3 undisturbed soil cores both at saturation and after oven drying at 105°C for48h. We deduced Ǿ from the mass of water needed to fill sample pores. We calculated the air-filled porosity (ε) as the difference between Ǿ and volumetric water content (VWC). We calculated average and standard deviation values on triplicate samples for each depth.

The assessment of SWR curves was carried out following the widely used pressure plate technique: undisturbed soil samples were submitted to several increasing and discrete pressure values inside a closed chamber, with a precise monitoring of soil water content for each pressure level (Richards and Fireman, 1943).We used undisturbed soil cores at 10, 25, 35, 50, 70 and 95 cm depth, with 3 replicates at each depth. We obtained the ε100 and b parameters of the Campbell (1974) SWR model by fitting the model to the SWR observations (Moldrup et al. 2000).

2.3. Monitoring ofsoil CO_2, water and temperature

We measured soil CO_2 concentrations using custom-built soil CO_2probes. The CO_2 sensor in the probe is based on the CARBOCAP® Single-Beam Dual Wavelength non-dispersive infra-red (NDIR)

technology (GMM221, Vaisala corp., Vantaa, Finland). The analytical precision is function of both the probe characteristic and the value of the observation. This can be calculated as the sum of1.5% of the measurement range and 2% of the observed value. The sampling head of the CO_2 probe is a cylinder of 18.5 mm diameter and 40 mm long, covered with a PTFE (polytetrafluoroethylene) membrane, enabling gas exchange and protection against water infiltration. Since the GMM221 sensors were not designed for wet soil conditions, the sensors were encapsulated into an additional perforated PVC tube, providing an additional protection against water (Fig. 1). This tubing method is an adaptation of the technique presented by Young et al. (2009). We inserted these tubes vertically into the soil, after creating boreholes with a diameter that equals the diameter of the PVC tubes. This approach avoids the need to backfill the bore hole, which will disturb the soil structure and diffusion process. Two rubber stoppers, one at 155 mm from the tube head, and another at the top of the tube, prevented atmospheric air from penetrating into the gas sampling volume. Petroleum jelly on these two rubber stoppers ensured a perfect air- and water-tightness and we verified this under laboratory conditions before using the probes. We used a nylon membrane to avoid soil particles entering the perforated tube and to limit further water infiltration.

We adjusted the concentration ranges of the CO_2 probe for each soil depth and for each slope position. This allowed an optimal fit of the probes to the local concentrations. Each probe has to characterize the entire range of values encountered during the seasons while at the same time; it should have a sufficiently narrow measurement range to ensure measurement precision. At the summit position, measurements ranged between 0-2 % at 12, 25, 45 cm depth and between 0-5 % at 85 cm depth. At the footslope position, measurements ranged between 0-5 % at 12 cm depth, between 0-10 % at 25 and 45 cm depth and between 0-20% at 85 cm depth.

To avoid vegetation growth and any autotrophic contribution to the soil respiration, we covered the measurement plots with a synthetic permeable geotextile during the complete measurement period. To increase the quality of the soil CO_2concentration data time-series, we removed observations where the battery voltage was lower than 11.5 V. We also corrected soil profile CO_2concentrations measurements for temperature variations using the empirical formulas described by Tang et al. (2003).

This allowed removing the impact of temperature on the CO_2 reading of the CO_2 probe, since the CARBOCAP® technology is temperature dependent. The probe manufacturer (Vaisala corp., Vantaa, Finland) provided probe specific parameters values for the correction formulas. We also obtained observations of surface CO_2 fluxes by means of a portable infra-red gas analyzer with an automated closed dynamic chamber (LI-8100A system, LI-COR, United-States), following Davidson et al. (2002). The sampling design of these surface chamber CO_2 fluxes measurements on the same study site has been described in Wiaux et al. (2014 b).

We monitored soil temperature using a thermistor probe (Therm107, Campbell Scientific Lt., UK). Analytical precision is 0.4°C. We monitored soil volumetric water content (VWC) using Time Domain Reflectrometry (TDR) probes based on Topp's equation (Topp et al., 1980) calibrated in the close vicinity of our study site (Heimovaara, 1993; Garré et al., 2008; Beff et al., 2013

We recorded water, temperature and CO_2 concentration profiles measurements with an automatic data logger (CR1000, Campbell Scientific Lt., UK), connected to a multiplexer (AM16/32, Campbell Scientific, Campbell Scientific Lt., UK).

2.4. Overall sampling design

The sampling design is shown in Fig. 4. At each of the 2 slope positions, we measured soil VWC and CO_2 concentrations profiles with 3 replicates on each measurement depth (Fig. 4). We averaged these triplicates, providing an average value for each soil depth and slope position. This allows to account for the spatial variability of VWC and CO_2 concentrations (Maier and Schack-Kirchner, 2014), by extending the measurement footprint to an area of c. 5 m^2.

18 VWC measurement points (6 soil depths, 3 replicates) were collected at each of the 2 slope positions. VWC was measured at depths of 10, 25, 35, 50, 70 and 95 cm (Fig. 4). CO_2 concentrations was measured at depths of 10, 25, 45 and 85 cm. Soil temperature was measured at the same depths (10, 25, 45, 85 cm) but without replicates (Fig. 4). Soil temperature and VWC profiles were calculated using a linear interpolation between the depth specific values within the profile. We kept the values

constant between the sampling point at the top of the profile and the soil surface. The estimation of CO_2 concentration profiles is described below (section 2.5).

In order to obtain an equilibrated soil environment around the soil VWC, temperature and CO_2 probes, measurements started 1 month after the installation of the probes. At the footslope position, hourly time-series of VWC, temperature and CO_2 concentrations were recorded from 12 May to 13 December 2012 and from 14 May to 22 November 2013. At the summit position, measurements were recorded for the period from the 2 June to 13 December 2012 and from the 14 June to 22 November 2013.

We also performed surface CO_2 fluxes measurements at 16 dates (profile and surface sampling time was within a 30 minutes time interval). Note that the averaged values of CO_2 concentration for each observation depth cover the same area as the IRGA chamber network located at the soil surface (Fig. 4). These reference surface CO_2 fluxes allowed calibrating parameters of the soil gas diffusion model, ensuring the accuracy of profile CO_2 fluxes (section 2.4).

We calculated soil temperature and VWC profiles using a linear interpolation between the depth specific values within the profile. We kept the values constant between the sampling point at the top of the profile and the soil surface.

2.5. Calculation of the CO_2 fluxes profiles

We calculated the CO_2flux using Fick's first law of diffusion according to the gradient method (Eq. 1, e.g. Maier and Schack-Kirchner, 2014):

$$F_{CO_2} = -D_s \frac{\partial CO_2}{\partial z} \qquad \text{(Eq. 1)}$$

Where F_{CO_2} is the soil CO_2 flux [µmol m^{-2} s^{-1}], D_s the diffusivity of CO_2 in soil [m^2 s^{-1}], CO_2 the soil CO_2 concentration [µmol m^{-3}], and $\frac{\partial CO_2}{\partial z}$ the vertical soil CO_2 gradient (with "z" representing the soil depth).

In order to calculate the vertical soil CO_2 gradient, we suggest an equation that accounts for curve concavity variations (Eq. 2). Variations in curve concavity in CO_2 concentration profiles have already

been reported in the literature (e.g. Maier and Schack-Kirchner, 2014). In this study, we built Eq.2 to consider this issue and improve the model fit to CO_2 concentration profiles. We evaluated the performance of this fitting by means of the regression coefficient (R^2). When the R^2 values were lower than a threshold value of 95%, we considered the CO_2 concentration profile as unreliable and we did not retain the resulting CO_2 fluxes in the final analysis.

$$CO_2(z) = 0.04 + A\left(\left(\frac{1}{1+e^{-\gamma_1 z}}\right) + \left(\frac{1}{1+e^{-\gamma_2(z-d)}}\right) - \left(\frac{1}{2} + \frac{1}{e^{\gamma_2 d}+1}\right)\right) \quad \text{(Eq. 2)}$$

where z is the soil depth [cm], d is the soil depth [cm] at which the sharpness of the curve changes due to a diffusion barrier, $\gamma_1$and γ_2 [cm^{-1}] are fitted parameters which characterize the sharpness of the curve, respectively above and below the soil depth d, and A [%]isa reference value used to definethe fitted asymptotic value of the CO_2 concentration at infinite depth. We fitted the A, d, $\gamma_1$and$\gamma_2$parameters for each CO_2-profile using the trust-region-reflective optimization algorithm in Matlab ©. The derivative of Eq. 2 provided the CO_2gradient ($\frac{\partial CO_2}{\partial z}$) used in Eq. 1 to calculated the CO_2 fluxes. The diffusivity of CO_2 in soil, D_s in Eq. 1), is a function of the diffusivity of CO_2 in free air (varying with temperature T and pressure, e.g. Davidson *et al*., 2006) and of the gas tortuosity factor (ξ) (Eq. 3):

$$D_s = \xi\, 1.47\, 10^{-5} \left(\frac{T+273}{273}\right)^{1.75} \quad \text{(Eq. 3)}$$

whereξ depends on soil physical and hydrological properties. We used the Moldrup et al. (2000) model (Eq. 4) which was shown to provide the most accurate and precise results (Davidson et al., 2006; Goffin et al., 2014);

$$\xi = (2{\varepsilon_{100}}^3 + 0.04\varepsilon_{100}) \left(\frac{\varepsilon}{\varepsilon_{100}}\right)^{2+3/b} \quad \text{(Eq. 4)}$$

where ξ is the gas tortuosity factor,ε[m^3 m^{-3}]is the soil air-filled porosity, b[-] is the slope of the Campbell (1974) soil water retention curve model between -100 and -500 cm H_2O water suction, and ε_{100}[m^3 m^{-3}]is the soil air-filled porosity at a soil water potential of -100 cm H_2O.

248 CO_2 fluxes, as assessed by the gradient based method, were calculated on an hourly time-scale, and
249 then integrated on a daily basis. Temperature, VWC, diffusivity and CO_2 concentration values were
250 also averaged on a daily basis.

251 In contrast to other studies (e.g. Pingintha et al., 2010; Turcu et al., 2005), we did not aggregate the
252 soil diffusivity coefficient for the entire soil profile or for an entire soil layer. We considered the
253 vertical distribution explicitly, and integrated Eq. 4 in the finite difference numerical solution of Eq. 1.
254 In this numerical integration, we used a depth increment of 0.1cm and constrained the surface CO_2
255 concentrations with atmospheric CO_2 levels (i.e.0.04%). In addition, and contrary to Goffin et al.
256 (2014) and Maier and Schack-Kirchner (2014), we did not calculate the CO_2 fluxes from each soil
257 slice based on the difference of CO_2 concentrations between the top and the bottom of soil horizons,
258 but we rather assessed a continuous profile of CO_2 fluxes and production.

259 ## 2.6. Calibration of the gradient-based CO_2 fluxes with direct observations at the
260 ## soil surface

261 We calibrated the diffusion model by adjusting the parameters related to the gas diffusion coefficient
262 (i.e. b and ε_{100}) in such a way that calculated fluxes fit instantaneous CO_2 fluxes observations at 16
263 dates spread along the measurement period. This calibration ensures the consistency, and consequently
264 the precision, of the calculated CO_2 fluxes. Comparing the gradient-based CO_2 fluxes with directly
265 measured IRGA CO_2 fluxes, we obtained a good precision with a R^2 of 92% for all soil profiles
266 together (Fig. 5). In addition, the slope of the fit (i.e. 1.05 and 1.22, respectively in 2012 and 2013,
267 Fig. 5) was used to correct the estimated fluxes. The comparison between gradient-based calculation
268 and observed surface CO_2 fluxes, which allowed the optimization of the calculated fluxes, is illustrated
269 in Fig. 5.

270 ## 2.7. Vertical partitioning of CO_2 fluxes

271 We partitioned the continuous CO_2 flux profiles obtained using Eq.2 into 10 slides of 10 centimeters
272 along the soil profile. For each soil slide, we calculated the difference between the top and bottom

fluxes. We divided this difference by the total CO_2 flux (e.g. the value at the soil surface). This provides the relative contribution in terms of both CO_2 production and transfer (in %) of each soil slide to the surface CO_2 flux (e.g. Goffin et al., 2014; Maier and Schack-Kirchner, 2014).

In order to allow an easy representation of the temporal dynamic of this vertical partitioning, we averaged values on a time-scale of one month and a half, representing the beginning or the end of a season. Standard deviation values reflect the variability overtime during each half season.

3. Results

3.1. Spatio-temporal analysis of measured soil variables

Fig. 6 to Fig. 10 respectively show the spatio-temporal variation of soil temperature, moisture, CO_2 fluxes, concentrations and diffusion. All these values correspond to in-situ measurements during a 6 month period in 2013. Similar measurements have been carried out in 2012 and display similar spatio-temporal trends (data not shown). Here, we focus on the temporal dynamics of the measured variables, as well as the shape of the vertical distribution along the soil profile. The relationship between these variables was previously analyzed in Wiaux et al. (2014b) and this is not further discussed here. It should be noted that the comparison of the profile distribution at different dates or of temporal dynamics at different depths is done in a qualitative manner.

During the observation period, the soil temperature (Fig. 6) shows a rather similar evolution at the summit and the footslope, although higher temperatures were observed at the summit profile for some shorter periods (e.g. day of year 180 to 220 where temperatures are approximately 2 to 3 °C higher). The mean daily temperatures at the soil surface ranges between 4°C to 28°C at the summit, and between4°C to 25°C at the footslope.

The space-time dynamics of the soil volumetric water content (VWC, Fig. 7) differ substantially between the summit and the footslope profiles. At the footslope, the observed soil VWC at different soil depths varied in a narrow range (0.36 to 0.39 cm^3 cm^{-3}). In contrast, soil VWC at the summitvariedbetween0.23 to 0.34 cm^3 cm^{-3}forthe plow layer (0-30cm depth) and higher values

298 (approximately 0.39 cm^3 cm^{-3}) were observed for the rest of the soil profile. The soil at the summit
299 position was the wettest during the early spring and the late autumn and driest in the summer. At the
300 footslope, soil VWC reached the saturation level in the early summer after an important rainfall event
301 and then slowly decreased until the early autumn and reached saturation again in the late autumn.

302 In contrast to the VWC, and as expected given the physical dependence of diffusivity to soil water
303 content (Eq. 4, section 2.5), the soil gas diffusivity (Fig. 8) reached its maximum value in the summer
304 at the summit while it was low at the footslope. Soil gas diffusivity was approximately 10 times lower
305 at the footslope than at the summit.

306 The soil CO_2concentrations at both the summit and the footslope increased gradually from spring to
307 late summer (Fig. 9a). Thereafter, concentrations dropped again and lowest values were observed in
308 the late autumn.

309 Theranges of CO_2 fluxes obtained for the footslope and summit profiles were very similar (Fig. 10a).
310 However, their temporal distribution was different: the periods characterized by high CO_2 fluxes did
311 not occur at the same time and had a different duration. More precisely, at the summit, peaks of CO_2
312 fluxes appear at the early summer and disappear after one month, while at the footslope, peaks of CO_2
313 fluxes appear at the early autumn and are 30% lower than at the summit but remain constant during
314 two months. For all soil profiles, CO_2 fluxes decreased with depth and reached null values at
315 approximately30 cm depth at the summit and at approximately 15 cm depth at the footslope.

316 ## 3.2. Shape and variability of CO_2concentrations and fluxes profiles

317 The observed soil CO_2 concentrations increased with soil depth (Fig. 9b), from the atmospheric value
318 of 0.04 % at the surface to concentrations which were two orders of magnitude higher at 100 cm depth
319 ($CO_2(z)$ in Eq.2). For the measurement period of 6 months considered here, CO_2concentration values
320 at 100 cm depth were three to four times higher at the footslope position than at the summit position.
321 In 2013, these values ranged from 0.86 to 3.46 % at the summit position and from 3.68 to 9.12 % at
322 the footslope position.

323 The observed CO_2 concentration profiles (Fig. 9b) followed a double exponential trend (Eq. 2).This
324 particular model built in this study to represent soil CO_2 concentration profiles (Eq. 2) fits our
325 observations relatively well, with regression coefficients ranging between 97 to 100%. These
326 exponential curve starts approximately at the middle of the profile, and is particularly pronounced at
327 the footslope, reflecting a shift of nearly 4% CO_2between 44 and 100 cm depth. Standard deviations
328 around averaged values of observed hourly CO_2 concentrations at each depth are given in Table 1. The
329 small-scale spatial variability is low relative to the mean values of CO_2 concentrations, the only
330 exception being the footslope at 25 cm depth where the maximum standard deviation exceeded the
331 maximum mean value.

332 The CO_2 fluxes (Fig. 10) were calculated based on both CO_2 concentrations and diffusivity. For all soil
333 profiles (Fig. 10a), CO_2 fluxes decreased with depth and reached null values at c.30 cm depth at the
334 summit and at c. 15 cm depth at the footslope.

335 3.3. Vertical partitioning of CO_2 fluxes

336 The distribution of the soil CO_2 fluxes in the profile is illustrated in Fig. 11. At the summit (Fig. 11a),
337 the relative contribution of the different soil layers was more dynamic in time, with a contribution of
338 the first ten centimeters of the soil profile ranging from 80 % at the late spring, decreasing to 60 % in
339 the early summer, and reaching 40 % from late summer to the late autumn. At the summit (Fig. 11a),
340 the first 30 centimeters of the soil profile significantly contributed to surface fluxes. This contribution
341 decreased with depth in the late spring and the early summer, but is homogeneously distributed with
342 depth for the rest of the time. At the summit (Fig. 11a), soil layers deeper than 30 cm depth sometimes
343 contributed for up to 20% of the total flux, especially in the autumn. At the footslope (Fig. 11b), 90 to
344 95 % of the surface CO_2 fluxes were generated in the first ten centimeters of the soil profile. The soil
345 layer between 10 and 20 cm contributed for only 5 to 10 %, and the deeper layers did not significantly
346 contribute to the surface fluxes.

4. Discussion

4.1. Soil physical control on CO_2 emissions

The observed differences between the footslope and summit soil profiles, in terms of the temporal evolution of surface soil CO_2 fluxes (Fig. 10), indicate that the controlling factors are not the same. At the summit, the evolution of surface soil CO_2 fluxes (Fig. 10) clearly follows the temperature variations (Fig. 6, maximum during the summer). At the footslope, the soil surface CO_2 flux was small even when temperature increased and remained relatively small throughout the summer period (Fig. 10). This is most likely related to the high VWC values observed at the footslope (Fig. 7), as it is well known that VWC negatively impacts soil CO_2 emissions (e.g. Webster et al., 2008b; Perrin et al., 2012; Wiaux et al., 2014b). More precisely, we suggest that VWC is not the only factor controlling CO_2 emissions at the footslope, but that the difference between the VWC and the water saturation level of the soil pore spaces, i.e. the water-filled pore spaces, also plays an important role. While the VWC at the footslope remained high throughout the year, we observed that the soil surface CO_2 flux dramatically increased when the air-filled pore spaces becomes high enough, which is illustrated by the gas diffusivity exceeding a threshold value of c. 0.1 $cm^2\ d^{-1}$ (i.e. from day 255 to 305 of year 2013, Fig. 10). Hence, we argue that the occasionally low CO_2 emissions at the footslope profile are related to the high VWC, as described in the literature by the bimodal effect of VWC on CO_2 emissions (e.g. Davidson et al., 1998; Perrin et al., 2004; Webster et al., 2008b; Castellano et al., 2011; Bauer et al., 2012; Wiaux et al., 2014b). Indeed, according to these authors, when a threshold VWC value is exceeded, this: (i) strongly limits the transfer of biotic CO_2 along the soil profile, and (ii) reduces the production of CO_2 in itself due to the lack of oxygen for the microbial community. In both cases, the lower CO_2 emissions at the footslope profile relative to the summit, are due to gas diffusion limitations (even indirectly in the case of oxygen lack), as also suggested by Ball (2013). This stands in sharp contrast to the summit profile where gas can easily diffuse throughout the year and along the entire soil profile (Fig. 8).

In the period preceding the important CO_2 emissions (i.e. from day 255 to 305 of year 2013, Fig. 10), the soil CO_2 cannot move along the soil profile and accumulates within soil pores. This results in an increase of the CO_2 concentration during the early and the late summer, especially below 50 cm depth (Fig. 9), where a compacted soil layer appears (see porosity profile in Fig. 1). This suggests that gas diffusion barriers strongly impact the CO_2 concentration profile at the footslope. As a result of these gas diffusion barriers, 90 to 95% of fluxes occur from the top soil (i.e. the first 10 cm) at this location (Fig. 11).This suggests that contributions of deep soil layers could be higher without these diffusion barriers. This may occur in dry conditions where even compacted soil layers can display a low proportion of water in pore spaces. The permanently high water content (Fig. 7), at least during the period of observations, measured at this downslope location prevents the contribution of deeper soil layers. While this soil profile remains wet all the time, the temporal dynamics of VWC and gas diffusion at the footslope (Fig. 7-8)control the time-dynamic behavior of soil surface CO_2 fluxes (Fig. 10). This is in agreement with recent studies (e.g. Maier et al., 2011; Schmidt et al., 2011; Ball, 2013) that show that soil physical properties are key to understand the mechanisms regulating the soil gases emissions. Our study brings new insights by demonstrating the strong linkages between soil physical properties and CO_2 emissions based on in-situ and depth-explicit observations. However, further work is still needed to better understand the processes controlling microbial inhibition and the gas transfer inhibition incase of soil diffusion barriers.

As a consequence, we argue that the significantly higher CO_2 concentrations observed at the footslope, especially for deeper soil layers, are not only related to the large amount of labile OC that was found at this position (shown in Wiaux et al., 2014a,b), but more likely result from the long term accumulation (i.e. during periods with a very low diffusivity) of the CO_2 produced by the mineralization of this large labile OC stock. Maier et al. (2011) showed that the CO_2 efflux (observed CO_2 flux resulting from all transfer and production mechanisms together) can deviate in time from the instantaneous soil respiration (due to micro-organisms metabolic activity) because of the CO_2 storage into soil pore spaces. Hence, our data suggest that at the footslope, soil physical properties are the dominant control on surface CO_2 fluxes. In other words, while the footslope profile contains more labile OC in the

399 subsoil relative to the summit (Fig. 1, Wiaux et al., 2014a), there is a lower contribution from the
400 subsoil to the overall respiration fluxes due to physical limitations (both low diffusivity and lack of
401 O_2).

402 In summary, our study highlights that the mechanisms that govern soil surface CO_2 emissions are
403 highly variable in both space and time. On a well-drained soil at the summit of a hillslope, the
404 observed soil CO_2 emissions were directly related to soil microbial respiration and CO_2 production
405 (e.g.Wiaux et al., 2014b). However, at the footslope of the hillslope, which is characterized by a
406 different hydrological regime, we observed that the temporal dynamic of soil CO_2 emissions were
407 more closely related to physical transfer mechanisms: long periods of CO_2 production and
408 accumulation alternate with periods of important release at the soil surface. When considering a
409 situation where gas diffusion is limited, and as a result, also oxygen supply for micro-organisms is
410 low, we argue that oxygen concentration in soil pore spaces is not completely null. Hence, the
411 remaining oxygen allows CO_2 production through microbial respiration, especially at the footslope due
412 to the high amount of labile soil OC (Wiaux et al., 2014b).This CO_2 then accumulates under the soil
413 diffusion barriers. This accumulated CO_2 is then later emitted when VWC decreases under a threshold
414 value which allows a significant gas diffusion, as suggested by Maier et al. (2011) and Ball (2013).
415 The main implication of these observations is that if hydrologic regimes change and that footslope
416 soils become drier (reaching moisture conditions favorable for micro-organisms respiration and gas
417 transfer), there is a large amount of potentially easily decomposable OC stored at depth that can
418 suddenly decompose and be emitted to the atmosphere.

419 ## 4.2. Soil organic carbon storage in downslope deposits

420 The soil respiration rate can be interpreted as an indicator of soil OC persistence (e.g. Gregorich et al.,
421 1994; Wiaux et al., 2014a,b). However, a further analysis of what occurs along the soil profile is
422 needed to thoroughly answer the question of the persistence of OC. The vertical partitioning of the soil
423 CO_2 fluxes, as illustrated in Fig.11, shows that during the observation period, 90 to 95 % of the surface
424 CO_2 flux originated from the first ten centimeters of the soil profile at the footslope. Given the

important amount of OC until up to 100 cm depth in our study site (Fig. 1,Wiaux et al., 2014 a), this observation is not in agreement with the study of Goffin et al. (2014), who suggested that the relative contribution of asoil layer to the surface CO_2 fluxes is related to OC distribution along the soil profile. However, while similarities exist in the physical controls and the method used to calculate the vertical partitioning, the study of Goffin et al. (2014) reports on CO_2 production in forest soils. Comparing forest and crop soils is difficult because of the important part of the autotrophic respiration originates from roots in forest while this is less important in cropland soils (e.g. Davidson et al., 1998; Epron et al., 2006; Martin and Bolstad, 2009; Webster et al., 2008b; Goffin et al., 2014). Hence, in the case of forest ecosystems, the dense roots network in soil creates interferences when measuring heterotrophic CO_2 fluxes, and this has been shown to explain an important part of the vertical distribution of CO_2 production along soil profiles in forest ecosystems (Goffin et al., 2014).In addition, the estimation of CO_2 production in forest soils is more difficult as turbulent advection needs to be accounted for (i.e. the predominance of non-diffusive transport in the litter layer, Goffin et al., 2014). All these elements make a direct and quantitative comparison between forest and agro-ecosystems difficult. However, we can observe some qualitative similarities between our observations and those of Goffin et al. (2014) in forest soils: (i) surface soil VWC values and dynamics were shown to be a critical factor in accurately estimating topsoil CO_2 production, and (ii) the vertical distribution of CO_2 concentration increased with depth while CO_2 production decreased with depth. In addition, the substantial contribution of the upper soil layers found here was not related to higher temperatures (Fig. 6), contrary to what was suggested by Takahashi et al. (2004). According to the CO_2 concentration and diffusivity profiles (Fig. 8), the relative contribution of the soil layers to the surface CO_2 flux is more likely governed by soil physical controls (Ball, 2013) rather than by biological production depending on thermal energy and OC substrate. Here, soil gas diffusivity strongly decreases from 10 to 40 cm depth (where diffusivity is null) at the two slope positions, and the profile of CO_2 concentration displays no gradient between 10 and 40 cm depth, particularly at the footslope (Fig. 9).

Our data showed that despite the fact that the footslope profiles generates CO_2 fluxes which exceed those observed at the summit position (demonstrated in Wiaux et al., 2014b), the contribution of soil

452 layers below10 cm depth is very small(Fig. 11). The OC in the top layer of the soil profile (i.e.0-10
453 cm) contributed for approximately 90% of the total CO_2 flux at the footslope position (Fig. 11). This
454 can be explained by environmental conditions specific to this 0-10 cm layer playing in favor of both
455 microbial respiration and gas diffusion. There are no limitations related to both diffusion barriers and
456 access to the oxygen close to the soil surface. Hence, the only impact of soil VWC on soil respiration
457 is its positive effect as it provides a more easy access for soil micro-organisms to their OC substrate,
458 and to the enhancement of their metabolic activities by water (Akinremi et al., 1999; Castellano et al.,
459 2011; Herbst et al., 2008; Howard and Howard, 1993; Šimůnek and Suarez, 1993). The combination
460 of this high amount and high quality of soil OC (Fig. 1, as described by Wiaux et al., 2014a) with this
461 net positive effect of soil VWC results in a strong increase of microbial respiration rates.

462 Finally, our results suggest that buried soil OC in colluvial deposits is effectively protected from
463 mineralization below 10 cm depth, which corroborates the assumption of a long-term stabilization of
464 buried OC in colluvial soils as suggested in the literature (e.g. Doetterl et al., 2012; Berhe et al., 2008,
465 2012a).This also corroborates the notion of Schmidt et al. (2011) suggesting that deep soil OC may be
466 protected because of unfavorable physical conditions rather than substrate limitations.

467 ## 5. Conclusion

468 In this study, we evaluated the factors controlling soil carbon dioxide fluxes for two soil profiles along
469 a hillslope characterized by contrasting physical and chemical characteristics. At the summit position
470 of the hillslope, the time course of surface soil CO_2 fluxes was strongly related to soil temperature and
471 maximum CO_2 fluxes were observed during the summer. Here, the observed soil CO_2 emissions are
472 directly related to soil micro-organisms respiration and associated to biotic CO_2 production. In
473 contrast, the higherlevels of water filled pore space observed at the footslope profiles strongly limited
474 the transfer of biotic CO_2 throughout the soil profile and likely the transfer of O_2 to deeper soil depths.
475 The soil surface CO_2 flux increased substantially during short periods when the gas diffusivity
476 exceeded a threshold value related to sufficient air-filled pore spaces. As a result, the time course of
477 observed soil CO_2 emissions was to a large extent explained by physical transfer mechanisms: long
478 periods of accumulation alternate with shorter periods of important CO_2release. The vertical

partitioning of the soil CO_2 fluxes for the footslope profiles showed that, during the observation period, 90 to 95 % of the surface CO_2 fluxes originated from the first 10 centimeters of the soil profile. This study highlights the need to consider soil physical properties and their dynamics when estimating and modeling soil CO_2 emissions..When considering changes in hydrologic regimes, e.g. the footslope soils become drier (reaching moisture conditions favorable for micro-organisms respiration and gas transfer), there is a large amount of potentially easily decomposable OC stored at depth that can result in an additional emission of C to the atmosphere.

Author contribution

F.W. designed the experiments, and carried out the research. M.V., K.V.O. and F.W. analyzed the results. F.W. wrote the main part of the paper and prepared the manuscript with contributions from all co-authors.

Acknowledgement

This study was funded by the Fonds National pour la Recherche Scientifique(FNRS, Belgium, convention n° 1.A306.12) and by the Fonds de la Recherche Fondamentale Collective (FRFC, convention n° 2.4590.12). F.W. and K.V.O. are supported by the FNRS. We thank the technician team of the UCL, especially F. Laurent for his help and ideas in establishing the experimental setup for in-situ soil CO_2 concentration profile measurements, and S. François for the field campaigns of soil surface respiration measurements during more than 2 years. We kindly acknowledge Dr. J. Gillabel, from the Katholiek Universiteit van Leuven (Belgium), for hisvaluablescientific and technical advice. The experimental design illsutrated on Fig. 4has been inspired by his PhD thesis (non peer-reviewed publication).

References

Akinremi, O., McGinn, S., McLean, H., 1999.Effects of soil temperature and moisture on soil respiration in barley and fallow plots. Canadian Journal of Soil Science 79, 5-13.

Ball, B.C., 2013. Soil structure and greenhouse gas emissions: A synthesis of 20 years of experimentation. European Journal of Soil Science 64, 357-373.

505 Bauer, J., Weihermüller, L., Huisman, J.A., Herbst, M., Graf, A., Séquaris, J.M., Vereecken, H.
506 (2012). Inverse determination of heterotrophic soil respiration response to temperature and
507 water content under field conditions. Biogeochemistry 108, 119-134.

508 Beff, L., Günther, T., Vandoorne, B., Couvreur, V., Javaux, M. (2013). Three-dimensional
509 monitoring of soil water content in a maize field using Electrical Resistivity Tomography.
510 Hydrology and Earth System Sciences17, 595-609.

511 Berhe, A.A., Harden, J.W., Torn, M.S., Harte, J., 2008. Linking soil organic matter dynamics and
512 erosion-induced terrestrial carbon sequestration at different landform positions. J.
513 Geophys. Res. 113, G04039.

514 Berhe, A.A., Harden, J.W., Torn, M.S., Kleber, M., Burton, S.D., Harte, J., 2012.Persistence of soil
515 organic matter in eroding versus depositional landform positions. J. Geophys. Res. 117,
516 G02019.

517 Berhe, A.A., Kleber, M., 2013. Erosion, deposition, and the persistence of soil organic matter:
518 Mechanistic considerations and problems with terminology. Earth Surface Processes and
519 Landforms 38, 908-912.

520 Brahy, V., Deckers, J., Delvaux, B., 2002. Estimation of soil weathering stage and acid neutralizing
521 capacity in a toposequenceLuvisol–Cambisol on loess under deciduous forest in Belgium.
522 European Journal of Soil Science, 51, 1-13.

523 CAMPBELL, G.S., 1974. A Simple Method for Determining Unsaturated Conductivity From
524 Moisture Retention Data. Soil Science 117, 311-314.

525 Castellano, M.J., Schmidt, J.P., Kaye, J.P., Walker, C., Graham, C.B., Lin, H., Dell, C., 2011.
526 Hydrological controls on heterotrophic soil respiration across an agricultural landscape.
527 Geoderma 162, 273-280.

528 Chaopricha, N.T., Marín-Spiotta, E., 2014. Soil burial contributes to deep soil organic carbon
529 storage. Soil Biology and Biochemistry 69, 251-264.

530 Dai, Z., Trettin, C.C., Li, C., Li, H., Sun, G., Amatya, D.M., 2012. Effect of assessment scale on
531 spatial and temporal variations in CH 4, CO 2, and N 2O fluxes in a forested Wetland. Water,
532 Air, and Soil Pollution 223, 253-265.

533 Davidson, E.A., Belk, E., Boone, R.D. 1998. Soil water content and temperature as independent or
534 confounded factors controlling soil respiration in a temperate mixed hardwood forest. Global
535 Change Biology 4, 217-227.

536 Davidson, E.A., Janssens, I.A. 2006. Temperature sensitivity of soil carbon decomposition and
537 feedbacks to climate change.Nature 440, 165-173.

538 Davidson, E.A., Savage, K., Verchot, L.V., Navarro, R., 2002. Minimizing artifacts and biases
539 in chamber-based measurements of soil respiration. Agricultural and Forest Meteorology 113,
540 21-37.

541 Davidson, E.A., Savage, K.E., Trumbore, S.E., Borken, W., 2006. Vertical partitioning of CO_2
542 production within a temperate forest soil. Global Change Biology 12, 944-956.

543 Doetterl, S., Six, J., Van Wesemael, B., Van Oost, K., 2012. Carbon cycling in eroding landscapes:
544 Geomorphic controls on soil organic C pool composition and C stabilization. Global Change
545 Biology 18, 2218-2232.

546 Epron, D., Bosc, A., Bonal, D., Freycon, V., 2006. Spatial variation of soil respiration across a
547 topographic gradient in a tropical rain forest in French Guiana. Journal of Tropical Ecology
548 22, 565-574.

549 Eswaran, H., Van Den Berg, E., Reich, P., 1993. Organic carbon in soils of the World. Soil
550 Science Society of America Journal 57, 192-194.

551 Eugster, W., et al., 2010. Management effects on European cropland respiration. Agriculture,
552 Ecosystems & Environment 139, 346-362.

553 Fiener, P., Dlugoß, V., Korres, W., Schneider, K. 2012. Spatial variability of soil respiration in a
554 small agricultural watershed - Are patterns of soil redistribution important? CATENA 94, 3-
555 16.

556 Frey, S. D., Lee, J., Melillo, J. M., & Six, J. 2013. The temperature response of soil microbial
557 efficiency and its feedback to climate. Nature Climate Change, 3(4), 395-398.

558 Gallagher, M., Doherty, J., 2007. Parameter estimation and uncertainty analysis for a watershed
559 model. Environmental Modelling & Software 22, 1000-1020.
560
561 Garr´e, S., Huisman, S., andWeihermüller, L.: Manual for TDR calibration, Agrosphere Institute, ICG
562 IV, ForschungszentrumJülichGmbH, 52425 Jülich, Germany, 1–18, 2008.
563
564 Goffin, S., Aubinet, M., Maier, M., Plain, C., Schack-Kirchner, H., Longdoz, B., 2014.
565 Characterization of the soil CO2 production and its carbon isotope composition in forest soil
566 layers using the flux-gradient approach. Agricultural and Forest Meteorology 188, 45-57.

567 Gregorich, E.G., Carter, M.R., Angers, D.A., Monreal, C.M., Ellert, B.H., 1994.Towards a
568 minimum data set to assess soil organic matter quality in agricultural soils. Canadian Journal
569 of Soil Science 74, 367-385.

570 Heimovaara, T. J.(1993). Design of triple-wire time domain reflectometry probes in practice and
571 theory, Soil Sci. Soc. Am. J 57, 1410–1417.

572 Herbst, M., Hellebrand, H.J., Bauer, J., Huisman, J.A., Simunek, J., Weihermuller, L., Graf, A.,
573 Vanderborght, J., Vereecken, H., 2008. Multiyear heterotrophic soil respiration: Evaluation of
574 a coupled CO2 transport and carbon turnover model. Ecological Modelling 214, 271-283.

575 Houghton, R.A. (2003). Why are estimates of the terrestrial carbon balance so different?
576 Global Change Biology 9, 500-509.

577 Howard, D.M., Howard, P.J.A., 1993. Relationships between co2 evolution, moisture content and
578 temperature for a range of soil types.Soil Biology and Biochemistry 25, 1537- 1546.

579 IPCC, 1990.Detection of the greenhouse effect in the observations. Climate Change: The IPCC
580 Scientific Assessment (Wigley, TML, Barnett, TP), 239-256.

581 IPCC, 1992. Climate change 1992: the supplementary report to the IPCC scientific assessment
582 (Houghton, J.T., Callander, B.A.). Cambridge Univ Pr.

583 IUSS Working Group WRB. (2007). World Reference Base for Soil Resources 2006, first update
584 2007. World Soil Resources Reports No. 103. FAO, Rome.

585 Jacinthe, P. A. and R. Lal. 2001. A mass balance approach to assess carbon dioxide evolution during
586 erosional events. Land Degradation & Development 12:329-339.

587 Lal, R. (2003). Soil erosion and the global carbon budget.Environment International 29, 437- 450.

588 Maier, M., Schack-Kirchner, H., Hildebrand, E.E., Schindler, D., 2011. Soil CO2 efflux vs. soil
589 respiration: Implications for flux models. Agricultural and Forest Meteorology 151, 1723-
590 1730.
591
592 Maier, M., Schack-Kirchner, H., 2014. Using the gradient method to determine soil gas flux: A
593 review. Agricultural and Forest Meteorology 192–193, 78-95.
594
595 Martin, J.G., Bolstad, P.V., 2009. Variation of soil respiration at three spatial scales: Components
596 within measurements, intra-site variation and patterns on the landscape. Soil Biology and
597 Biochemistry 41, 530-543.

598 Moldrup, P., Olesen, T., Schjønning, P., Yamaguchi, T., Rolston, D.E., 2000.Predicting the gas
599 diffusion coefficient in undisturbed soil from soil water characteristics. Soil Science Society of
600 America Journal 64, 94-100.

601 Mualem, Y., 1976. A new model for predicting the hydraulic conductivity of unsaturated
602 porous media.Water Resources Research 12, 513-522.

603 Perrin, D., Laitat, É., Yernaux, M., Aubinet, M. 2004. Modélisation de la réponse des flux de
604 respiration d'un sol forestier selon les principales variables climatiques= Modelling of the
605 response of forest soil respiration fluxes to the main climatic variables. Biotechnologie,
606 agronomie, société et environnement 8, 15-25.

607 Peters, W. et al., 2010. Seven years of recent European net terrestrial carbon dioxide exchange
608 constrained by atmospheric observations. Global Change Biology 16, 1317-1337.

609 Pingintha, N., Leclerc, M.Y., Beasley, J.P., Zhang, G., Senthong, C., 2010. Assessment of the soil
610 CO_2 gradient method for soil CO_2 efflux measurements: Comparison of six models in the
611 calculation of the relative gas diffusion coefficient. Tellus, Series B: Chemical and Physical
612 Meteorology 62, 47-58.

613 Quinton, J.N., Govers, G., Van Oost, K., Bardgett, R.D., 2010. The impact of agricultural soil
614 erosion on biogeochemical cycling. Nature Geoscience 3, 311-314.

615 Reicosky, D.C., Lindstrom, M.J., Schumacher, T.E., Lobb, D.E., Malo, D.D., 2005. Tillage-
616 induced CO2 loss across an eroded landscape. Soil and Tillage Research 81, 183-194.

617 Richards, L. A., & Fireman, M. 1943. Pressure-plate apparatus for measuring moisture sorption and
618 transmission by soils. Soil Science, 56(6), 395-404.

619 Rommens, T., Verstraeten, G., Poesen, J., Govers, G., Van Rompaey, A., Peeters, I., Lang, A., 2005.
620 Soil erosion and sediment deposition in the Belgian loess belt during the Holocene:
621 Establishing a sediment budget for a small agricultural catchment. Holocene 15, 1032-1043.

622 Rumpel, C., Kögel-Knabner, I., 2011. Deep soil organic matter—a key but poorly understood
623 component of terrestrial C cycle. Plant and Soil 338, 143-158.

624 Schmidt, M.W.I., Torn, M.S., Abiven, S., et al. 2011. Persistence of soil organic matter as an
625 ecosystem property. Nature478, 49-56.

626 Šimůnek, J., Suarez, D.L., 1993.Modeling of carbon dioxide transport and production in soil: 1.
627 Model development. Water Resources Research 29, 487-497.

628 Smith, S.V., Sleezer, R.O., Renwick, W.H., Buddemeier, R.W., 2005. Fates of Eroded Soil
629 Organic Carbon: Mississippi Basin Case Study. Ecological Applications 15, 1929- 1940.

630 Stallard, R.F., 1998. Terrestrial sedimentation and the carbon cycle: Coupling weathering and
631 erosion to carbon burial. Global Biogeochemical Cycles 12, 231-257.

632 Tang, J.W., Baldocchi, D.D., Qi, Y., Xu, L.K., 2003. Assessing soil CO2 efflux using continuous
633 measurements of CO2 profiles in soils with small solid-state sensors. Agricultural and
634 Forest Meteorology 118, 207-220.

635 Takahashi, A., Hiyama, T., Takahashi, H.A., Fukushima, Y., 2004. Analytical estimation of the
636 vertical distribution of CO2 production within soil: application to a Japanese temperate forest.
637 Agricultural and Forest Meteorology 126, 223-235.

638 Topp, G.C., Davis, J.L., Annan, A.P., 1980. Electromagnetic determination of soil water
639 content: Measurements in coaxial transmission lines. Water Resources Research 16, 574-582.

640 Tran, A. P.,Bogaert, P.,Wiaux, F.,Vanclooster, M.,Lambot, S., 2015. High-resolution space–time
641 quantification of soil moisture along a hillslope using joint analysis of ground penetrating
642 radar and frequency domain reflectometry data, Journal of Hydrology 523, 252–261.

643 Trumbore, S.E., Czimczik, C.I., 2008. Geology - An uncertain future for soil carbon. Science 321,
644 1455-1456.

645 Turcu, V.E., Jones, S.B., Or, D., 2005.Continuous soil carbon dioxide and oxygen measurements
646 and estimation of gradient-based gaseous flux.Vadose Zone Journal 4, 1161- 1169.

647 Van Genuchten, M.T., 1980. A Closed-form Equation for Predicting the Hydraulic Conductivity of
648 Unsaturated Soils1. Soil Sci. Soc. Am. J. 44, 892-898.

649 Van Oost, K., Verstraeten, G., Doetterl, S., Notebaert, B., Wiaux, F., Broothaerts, N., Six, J., 2012.
650 Legacy of human-induced C erosion and burial on soil-atmosphere C exchange. Proceedings
651 of the National Academy of Sciences of the United States of America 109, 19492-19497.

652 Wang, Z., Van Oost, K., Lang, A., Quine, T., Clymans, W., Merckx, R., Notebaert, B., Govers, G.,
653 2014. The fate of buried organic carbon in colluvial soils: a long-term perspective.
654 Biogeosciences 11, 873-883.

655 Webster, K.L., Creed, I.F., Beall, F.D., Bourbonnière, R.A., 2008a. Sensitivity of catchment-
656 aggregated estimates of soil carbon dioxide efflux to topography under different
657 climatic conditions. Journal of Geophysical Research G: Biogeosciences 113.

658 Webster, K.L., Creed, I.F., Bourbonniere, R.A., Beall, F.D., 2008b. Controls on the heterogeneity of
659 soil respiration in a tolerant hardwood forest.Journal of Geophysical Research-Biogeosciences
660 113.

661 Wiaux, F., Cornelis, J.T., Cao, W., Vanclooster, M., Van Oost, K., 2014 a. Combined effect of
662 geomorphic and pedogenic processes on the distribution of soil organic carbon quality along
663 an eroding hillslope on loess soil. Geoderma 216, 36-47.

664 Wiaux, F., Vanclooster, M., Cornelis, J.T., Van Oost, K., 2014 b. Factors controlling soil organic
665 carbon persistence along an eroding hillslope on the loess belt. Soil Biology and Biochemistry 77,
666 187-196.

667 Yoo, K., Amundson, R., Heimsath, A.M., Dietrich, W.E., 2005. Erosion of upland hillslope soil
668 organic carbon: Coupling field measurements with a sediment transport model. Global
669 Biogeochemical Cycles 19.

670 Young, S.L., Pierce, F.J., Streubel, J.D., Collins, H.P., 2009. Performance of solid-state sensors for
671 continuous, real-time measurement of soil CO2 concentrations. Agronomy Journal 101,
672 1417-1420.

673

674

Tables

Table 1. Range of standard deviation (S.D.)and mean values of triplicated measured hourly CO_2 concentrations at each depth, both at the summit and at the footslope position. This range is indicated by minimum (Min) and maximum (Max) values encountered along time (hourly time series) during the 6 months measurement period. NI means No Information (i.e. due to a lack of replicates to allow reliable mean and S.D.).

	Summit position				Footslope position			
Soil depth [cm]	Min mean [%]	Max mean [%]	Min S.D. [%]	Max S.D. [%]	Min mean [%]	Max mean [%]	Min S.D. [%]	Max S.D. [%]
10	0.07	1.39	0.00	0.71	0.26	4.75	0.00	3.13
25	0.06	1.83	0.00	0.68	0.30	3.93	0.00	5.32
45	NI	NI	NI	NI	0.12	3.96	0.00	1.96
95	0.15	2.83	0.00	1.42	0.48	7.52	0.00	2.48

Figures

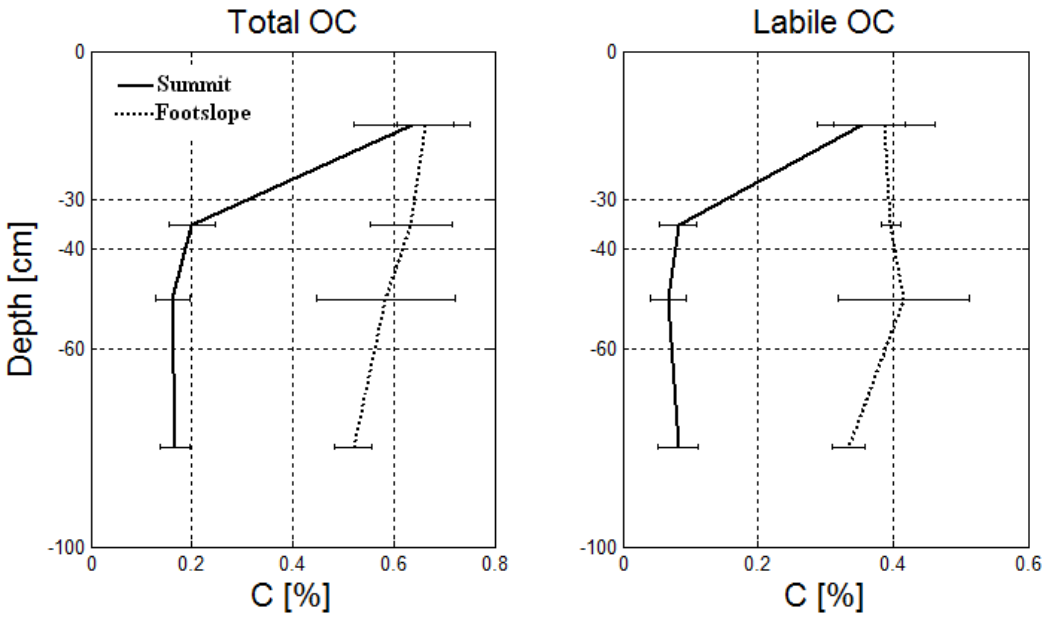

Fig. 1. Soil profiles (0-100 cm) of both soil total OC and labile OC pool concentrations [C%], at the summit and footslope positions. Error bars indicate 1 standard deviation (n≥3).

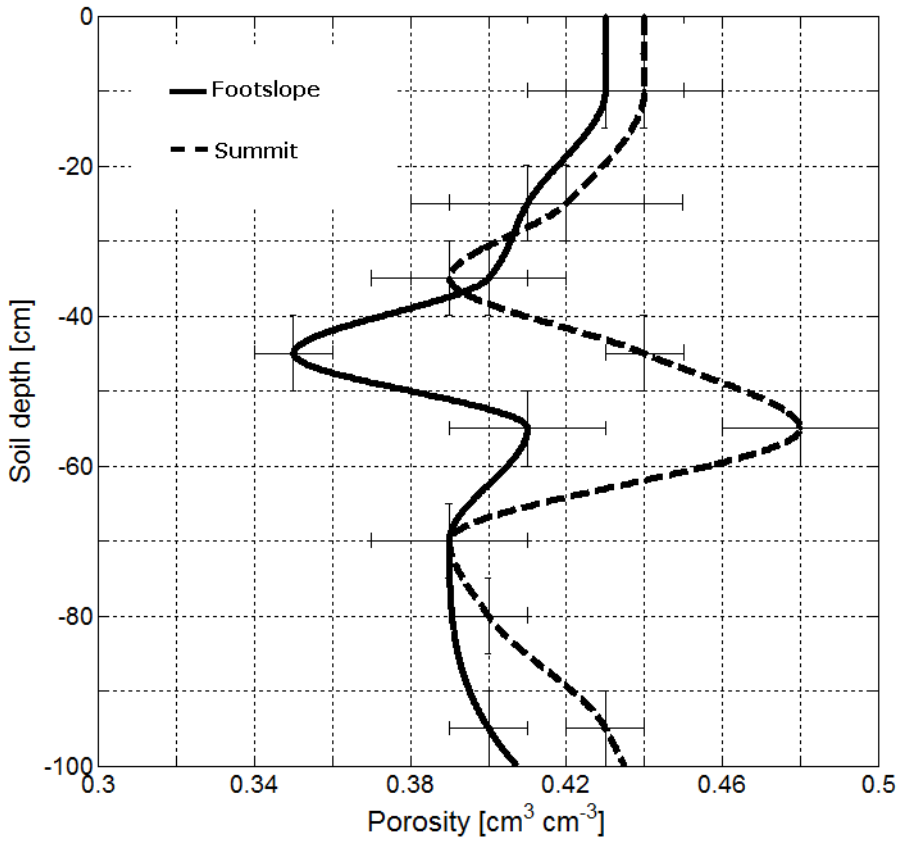

Fig. 2. Soil porosity profiles at the footslope (plain line) and at the summit (dashed line) positions. Error bars indicate 1 standard deviation (n≥3). Continuous lines are linearly interpolated values.

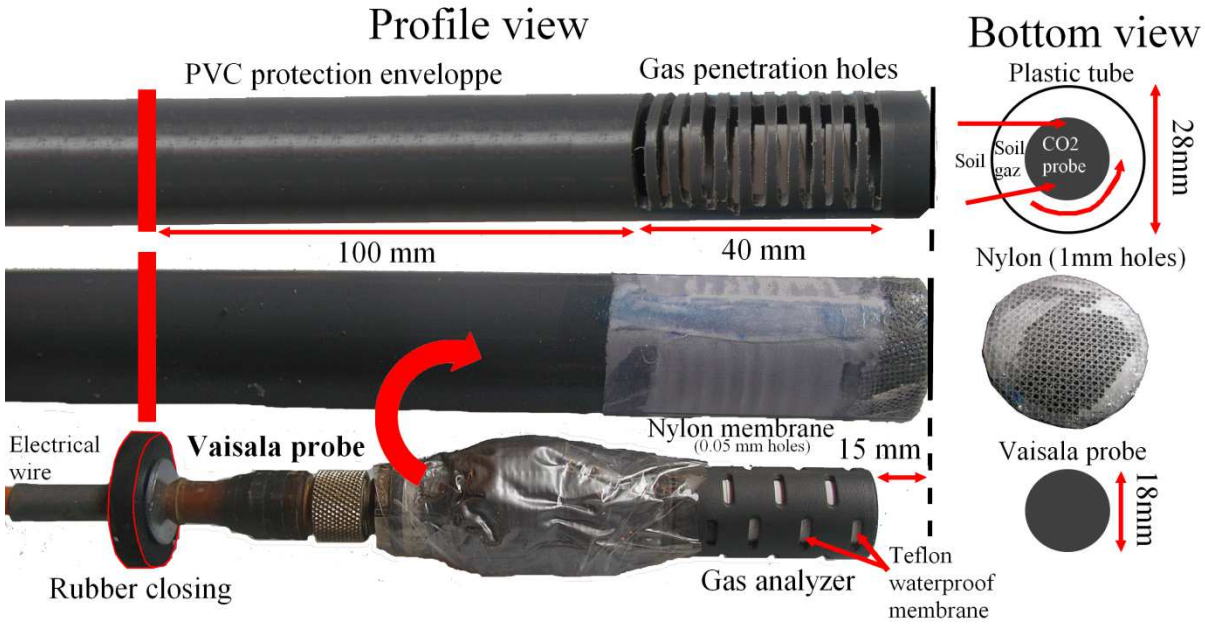

690

691 **Fig. 3. Description of the probes used for CO2 concentration measurements inside the soil.**

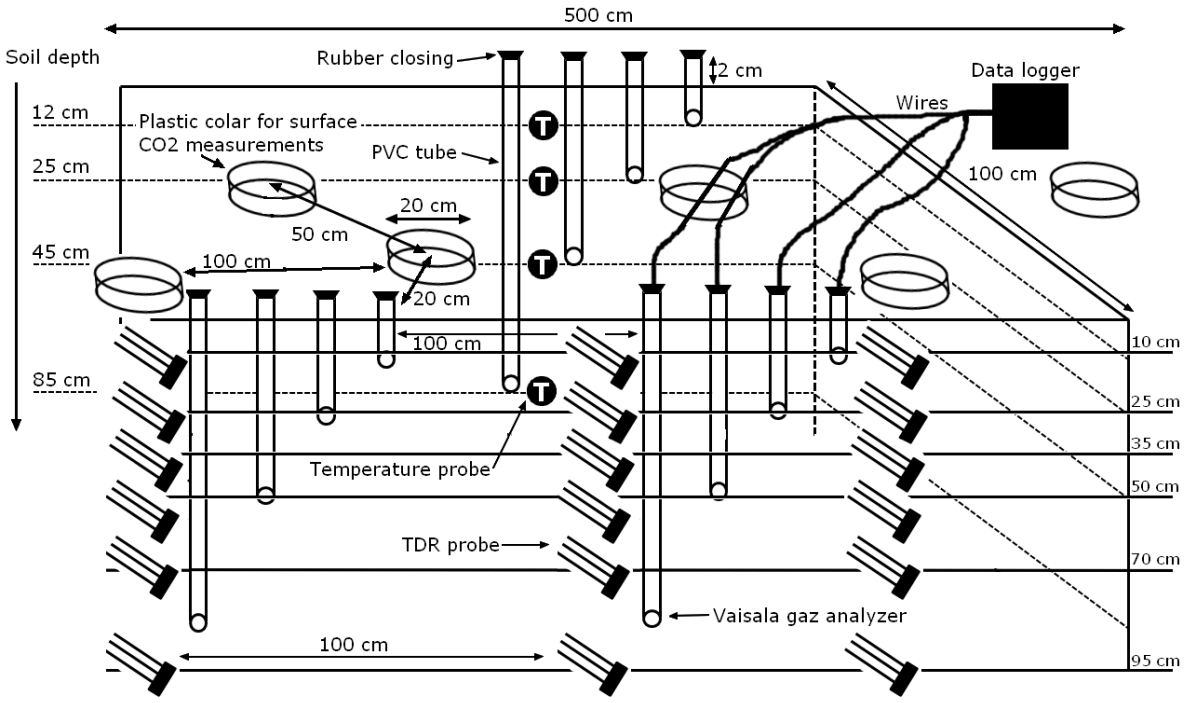

692

693 **Fig. 4.Schematic description of the experimental plot (sampling design) at each slope position showing how**
694 **temperature, VWC, CO_2 concentrations and CO_2fluxes probes collocate with each others. Probes have been inserted**
695 **at different locations both vertically and horizontally. Consequently, all of them are not in the same plane (i.e. depth**
696 **lines with axes labels on the right hand-side illustrate the foreground profile and depth lines with axes labels on the**
697 **left hand-side illustrate the background profile).**

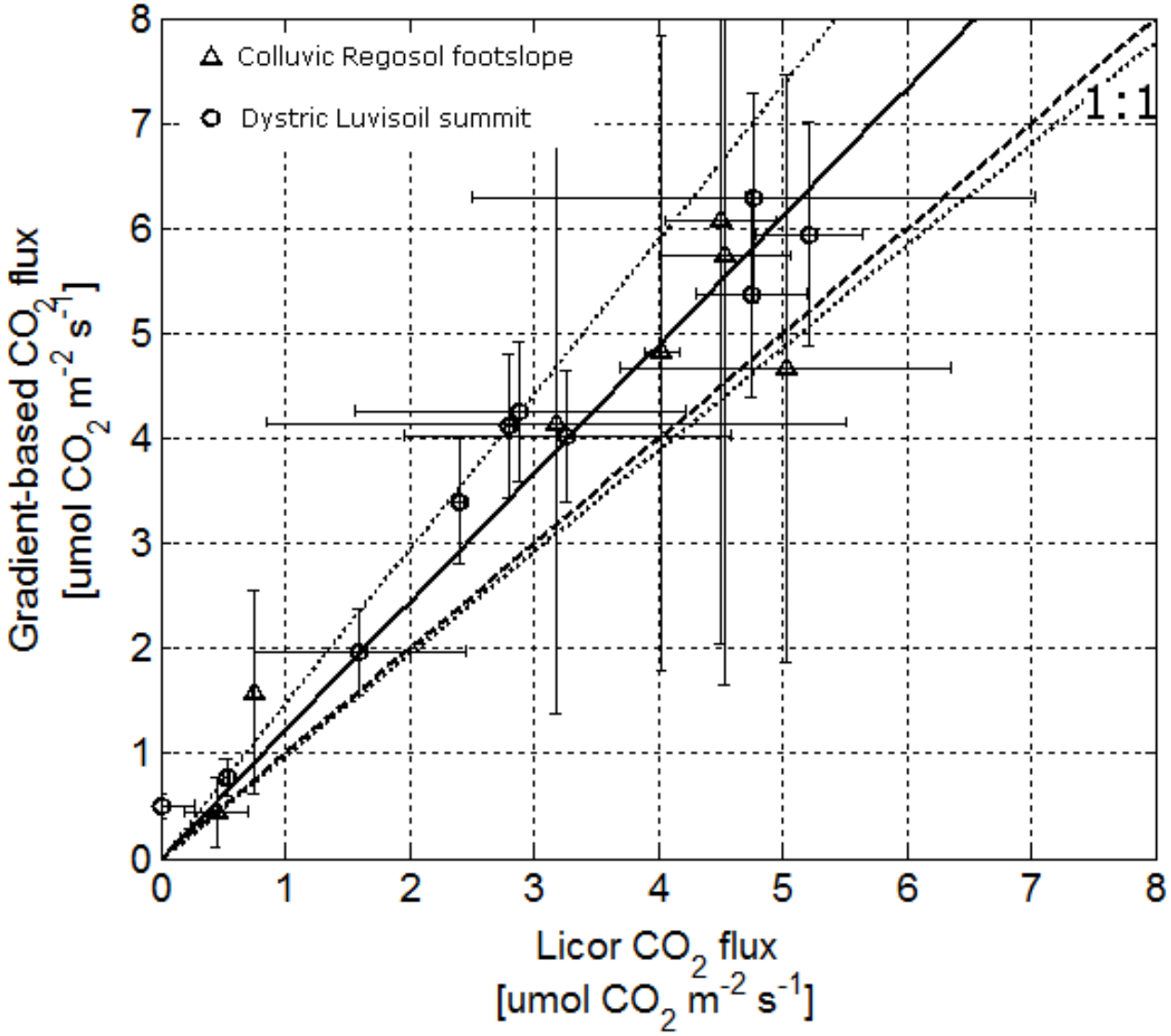

Fig. 5. Agreement between soil surface CO_2 fluxes directly measured with surface survey chambers (horizontal axes) and CO_2 fluxes calculated according to the gradient-based method (vertical axes) using the Moldrup et al (2000)diffusivity model. The plain straight line is the 1:1 ideal regression (perfect fit). The dashed straight line is the fitted regression. The dotted straight lines represent a 25% relative error interval around the fitted regression.

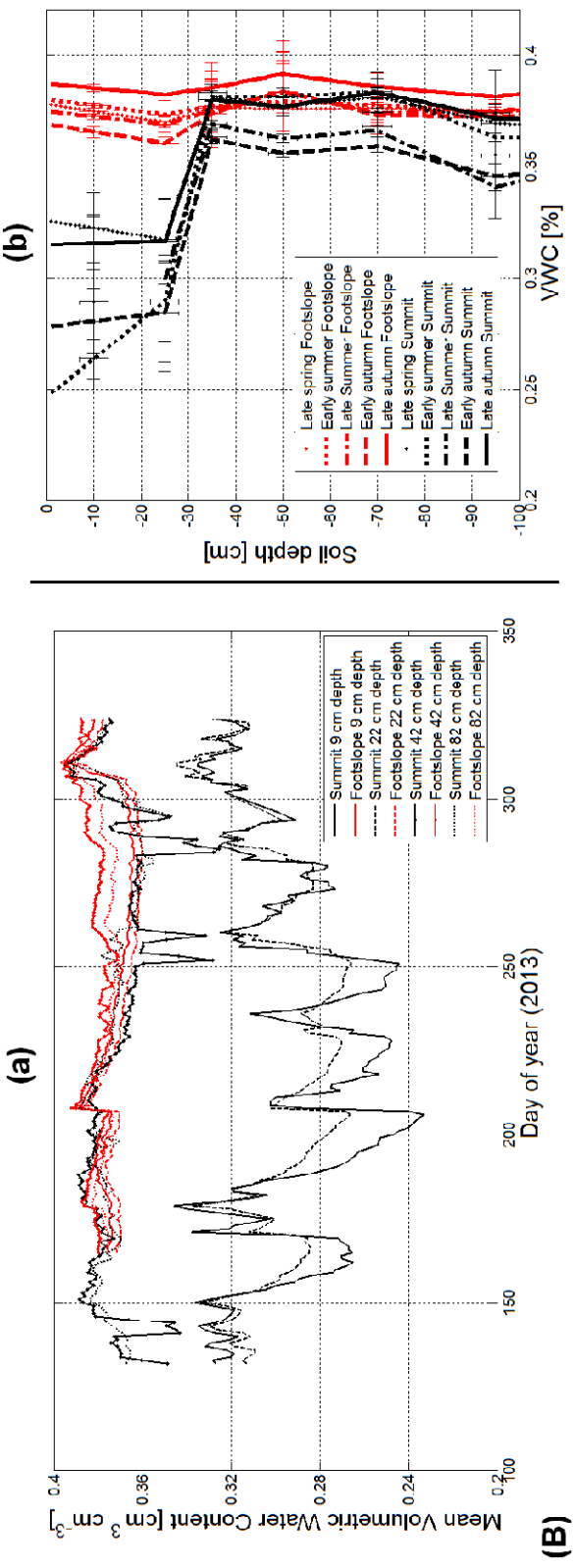

Fig. 6. Space-time dynamic of soil temperature at the summit (red) and the footslope (black) position in 2013: (a) time series at different depths; (b) Profile at different dates.

712

713 **Fig. 7. Space-time dynamic of soil moisture at the summit (red) and the footslope (black) position in 2013: (a) time**
714 **series at different depths; (b) Profile at different dates.**

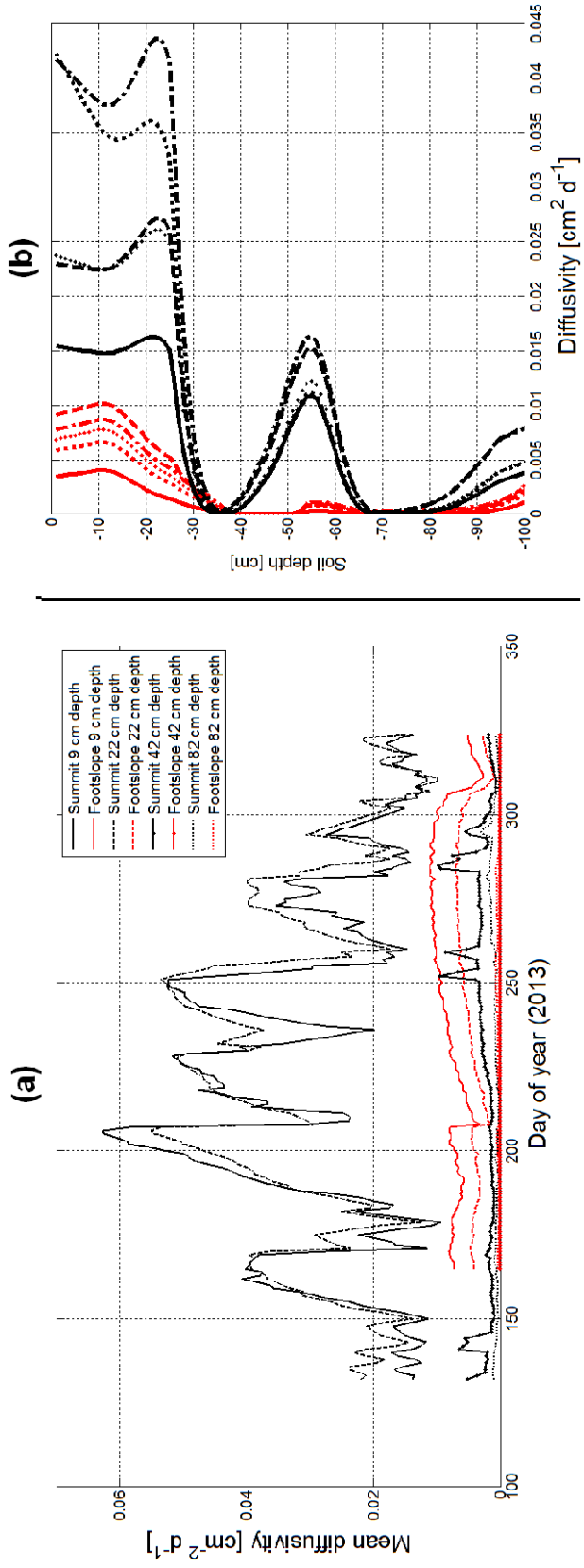

715

716 **Fig. 8. Space-time dynamic of soil CO_2diffusivity,at the summit (red) and the footslope (black) position in 2013: (a)**

717 **time series at different depths; (b) Profile at different dates.**

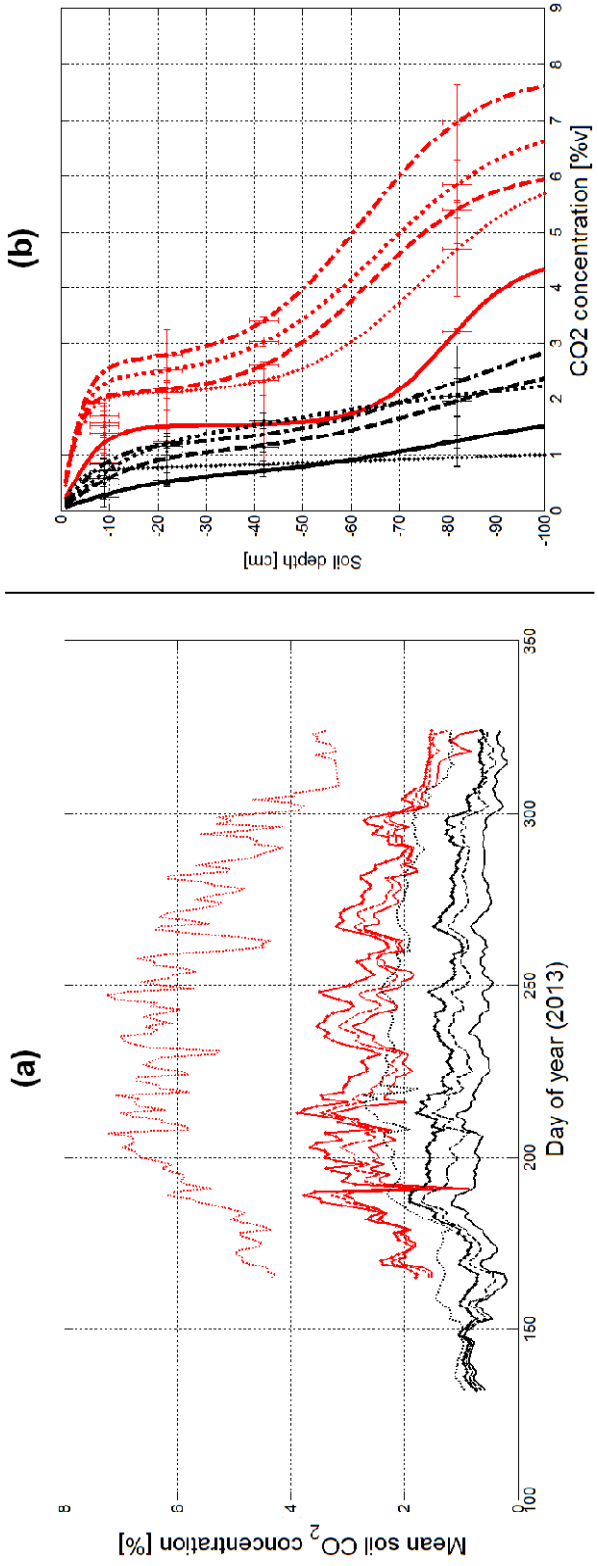

Fig. 9. Space-time dynamic of soil CO_2 concentrations, at the summit (red) and the footslope (black) position in 2013: (a) time series at different depths; (b) Profile at different dates.

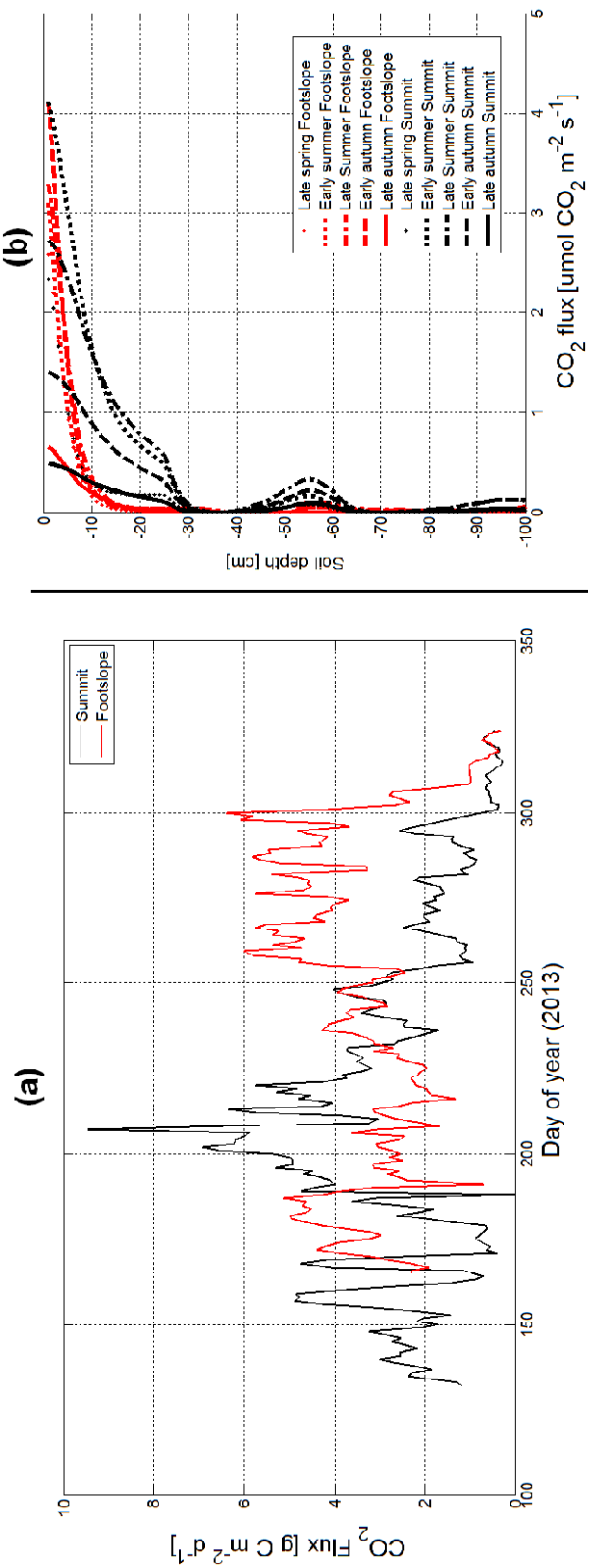

722
723

724 **Fig. 10. Space-time dynamic of soil CO_2 fluxes,at the summit (red) and the footslope (black) position in 2013: (a) time**

725 **series at different depths; (b) Profile at different dates.**

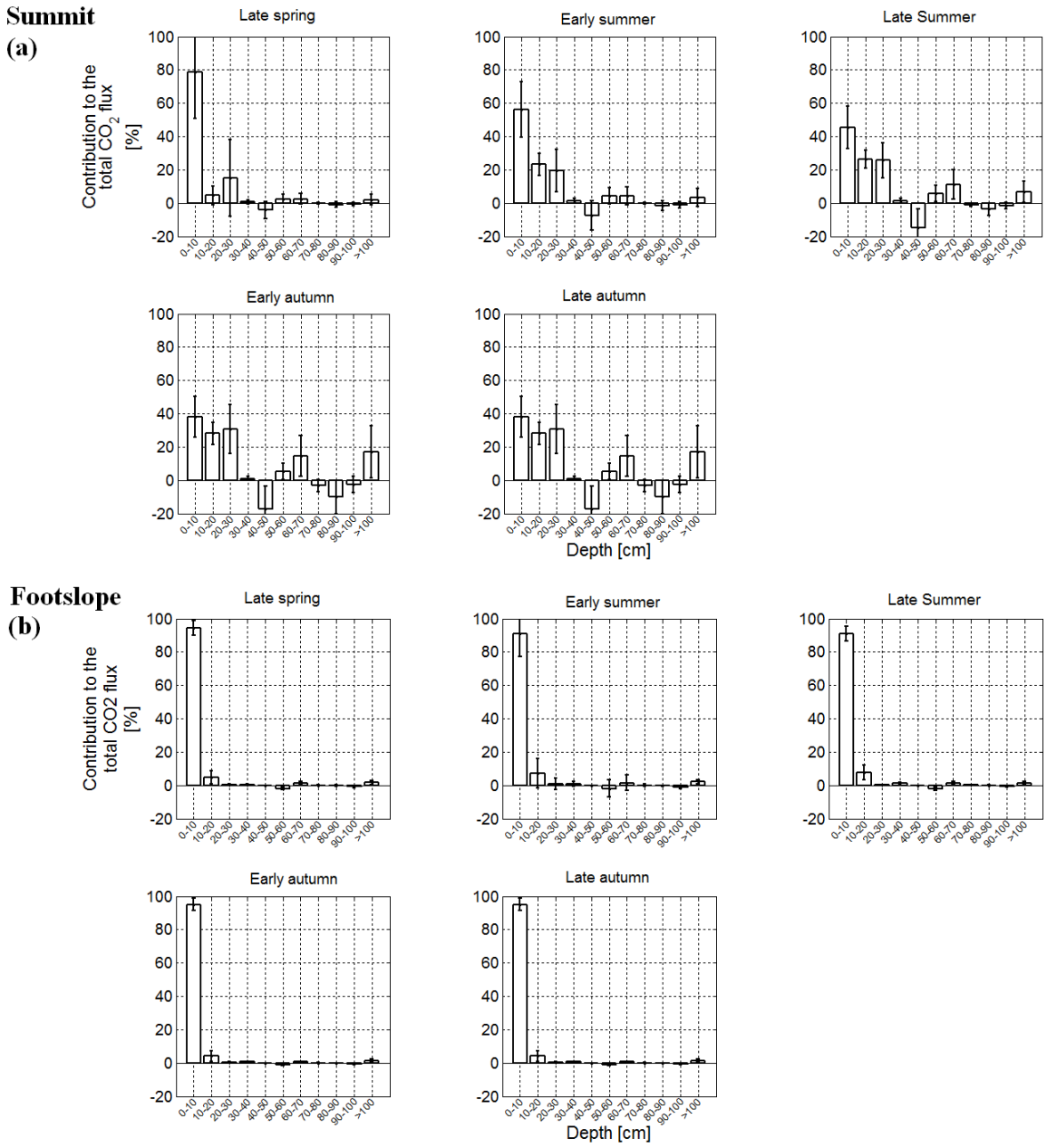

Fig. 11. Depth distribution of the relative contribution to soilsurface CO_2 fluxes in year 2013 averaged by semi-seasons (error bars represent the standard deviation of the time aggregation for each soil layer): (a) at the summit, and (b) at the footslope position.